# Molecular Dynamics Simulations of Hen Egg White Lysozyme Adsorption at a Charged Solid Surface

**ARTICLE** *in* THE JOURNAL OF PHYSICAL CHEMISTRY B · JULY 2009

Impact Factor: 3.3 · DOI: 10.1021/jp901521x · Source: PubMed



**2 AUTHORS:**

Karina Kubiak
University of Strathclyde
**20** PUBLICATIONS **232** CITATIONS
SEE PROFILE

Paul A. Mulheran
University of Strathclyde
**78** PUBLICATIONS **1,618** CITATIONS
SEE PROFILE

# Molecular Dynamics Simulations of Hen Egg White Lysozyme Adsorption at a Charged Solid Surface

**Karina Kubiak[†,‡] and Paul A. Mulheran*[,†]**

*Department of Chemical and Process Engineering, University of Strathclyde, James Weir Building, 75 Montrose Street, Glasgow G1 1XJ, United Kingdom, and Institute of Physics, Faculty of Physics, Astronomy and Informatics, Nicolaus Copernicus University, ul. Grudziadzka 5/7, 87-100 Torun, Poland*

*Received: February 19, 2009; Revised Manuscript Received: May 11, 2009*

Hen egg white lysozyme (HEWL) adsorption on negatively charged, hydrophilic surfaces has been investigated using atomistic molecular dynamics. Analysis of six 20 ns trajectories performed at pH 7 and ionic strength 0.02 M (NaCl) reveals that conformational alterations are required for HEWL adsorption, and that upon adsorption the protein loses some α-helical content. Simulations for a few different initial orientations show that the HEWL protein adsorbs on a flat surface with an angle between the protein long axis and the surface of about 45°. The main adsorption site is located on the N,C-terminal part of the HEWL surface; the major role is played by Lys1, Arg5, Arg14, and Arg128. Adsorption is not found with contrary orientations. Two additional 20 ns trajectories calculated with 0.5 M ionic strength suggest that the main force governing adsorption is electrostatic attraction between parts of the protein and the surface. A trajectory obtained for the protein situated inside a cubic box built from the charged surfaces shows that the adsorption pattern is different for flat and nonflat surfaces, and in particular, adsorption on the nonflat surface requires tertiary structure alterations and partial unfolding. The observed trends are consistent with both experimental and previous computational studies.

## Introduction

Interactions between proteins and hydrophobic or hydrophilic (solid or polymeric) surfaces are essential for a number of applications, such as food technology, protein separation methods, protein storage, drug delivery, contact lens optimization, surface functionalization, and medical implant design.[1−6] The understanding of the fundamental forces and processes involved in protein adsorption has a great importance in the control of interfacial protein behavior and could lead to the construction of new, biocompatible materials.

Denaturation of proteins by surfaces was discovered in 1941.[7] One of the most important surface active proteins is lysozyme. The hen egg white lysozyne (HEWL) protein was one of the first to have its three-dimensional structure determined by X-ray crystallography.[8] Lysozyme hydrolyzes either the $\beta$-(1−4)-linked homopolymer of *N*-acetylchitose (chitin) or the $\beta$-(1−4)-linked alternative copolymer composed of *N*-acetylchinose and *N*-acetylmuramic acid in the peptidoglycan component of the cell walls of Gram-positive bacteria, and could potentially be used as an anticancer drug and in HIV treatment.[9] Lysozyme may also be involved in the physiological control of melanin production in mosquitoes and mushrooms.[10]

It is widely known that protein adsorption is affected by numerous factors such as the protein shape and size, its hydrophobic or hydrophilic properties,[5,11,12] the pH of the solution,[12−15] its charge,[16] the ionic strength of the solution,[5,11,17] the solvent composition, the surface, the temperature[11] as well as protein composition.[18] Nevertheless, there is no consensus as to which of these factors is the crucial one. Current research focuses on determining whether the major driving force is electrostatics or hydrophobicity. HEWL adsorption on polymeric surfaces is probably driven by hydrophobic interactions,[12,19] while its adsorption on inorganic materials seems to be electrostatically driven.[16,20−23] For HEWL adsorption on solid surfaces such as gold,[24] magnetic particles ($Fe_3O_4$),[15,25] diamond nanocrystallites,[26] mica,[27−30] or silica,[31] the most important interactions are electrostatic attractions between the protein and the surface. The dependence on pH[13,14] and solvent ionic strength[5,11,21,32,33] provides further evidence for the role of electrostatic interactions. It is worth noting that a maximum adsorption value is reached at a pH near the isoelectric point of lysozyme,[12,23,25] and that an ionic strength higher than 0.5 M[32] prevents adsorption.

The extent and time (namely, before, during, or after adsorption) of the protein conformational changes due to adsorption are still under discussion. Some authors have reported that HEWL denaturation is necessary;[17,33−37] however, evidence for the tertiary structure being maintained has been found.[6,32,38−41] Adsorption induces an increase in random-coil and $\beta$-structure contents and a decrease in the α-helix content,[6,39] which indicates that HEWL adopts a more flexible conformation on the solid (silica) surface.[40] Very recently, a model for protein adsorption kinetics that considers these issues has been proposed.[42]

It is helpful to consider the lysozyme structure as an ellipsoid, which might in a simplistic view absorb in a "side-on" or "end-on" orientation with the major axis parallel or perpendicular to the surface. As can be seen in Figure 1a, the N-terminus lies more or less in the middle of one side of the protein surface parallel to the major axis, and the C-terminus is close by toward one end. On the opposite side, the active cleft is located toward the other end.

Experimental studies have confirmed "side-on" adsorption and the role of the N- and C-terminal parts of the protein.[6,32]

* To whom correspondence should be addressed. E-mail: paul.mulheran@strath.ac.uk.
† University of Strathclyde.
‡ Nicolaus Copernicus University.

10.1021/jp901521x CCC: $40.75 
Published on Web 06/11/2009

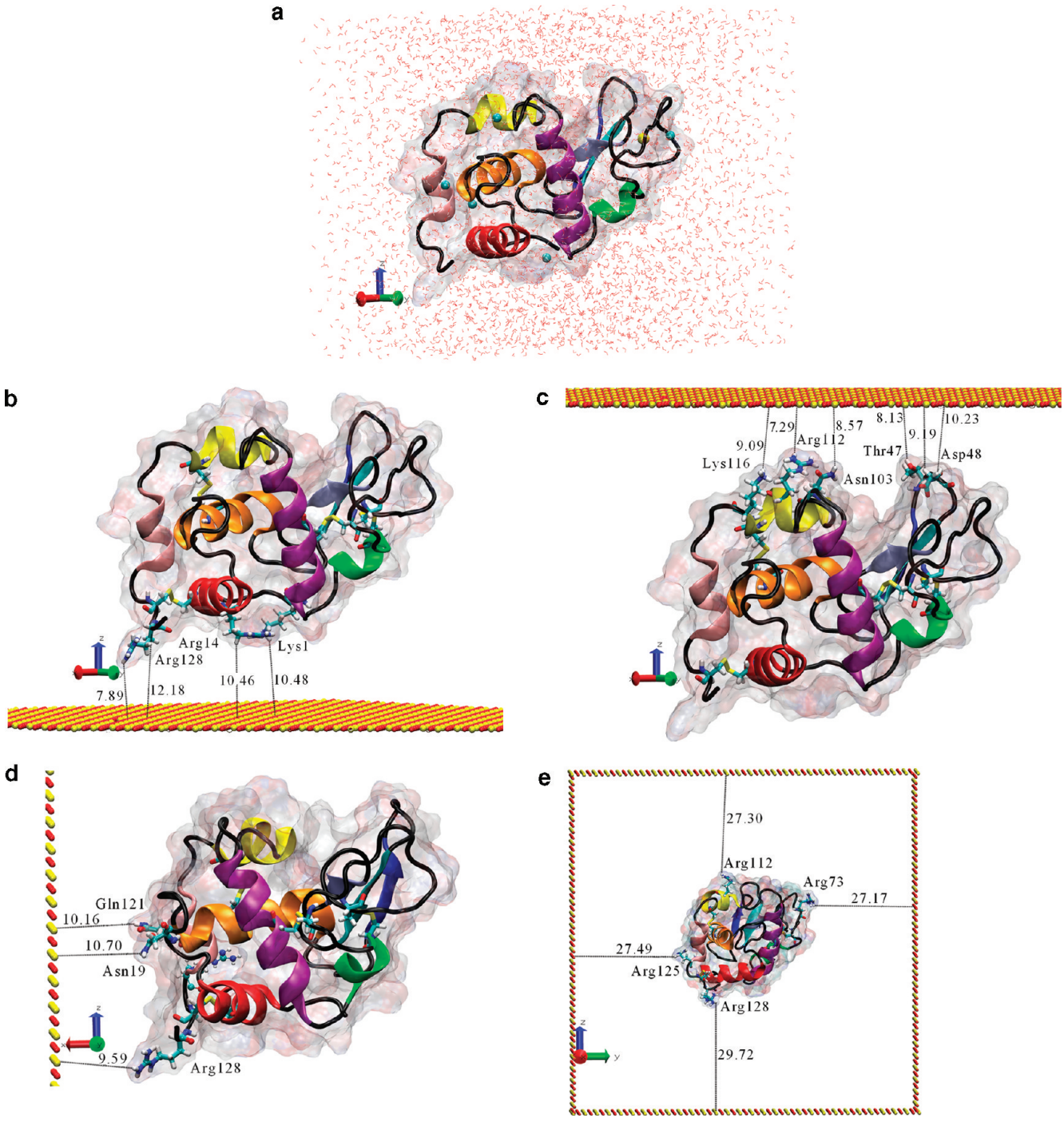


**Figure 1.** Initial systems: (a) isolated HEWL protein, (b) HEWL−surface system in orientation 1, (c) HEWL−surface system in orientation 2, (d) HEWL−surface system in orientation 3, and (e) HEWL−cage system, view from the front. Water molecules are shown just in the case of the isolated system; the surface is shown by the Corey−Pauling−Koltun model (CPK); oxygen and silicon atoms are indicated by red and yellow, respectively. The protein surface is indicated as a ghost surface; secondary structure elements are shown as a cartoon. In domain α, helix A (residues 5−16) is indicated by red, helix B (25−37) by orange, helix C (88−101) by purple, helix D (109−116) by yellow, and helix $3_{10}$ (120−125) by pink. In domain $\beta$, the $\beta$1 structure (residues 43−46) is indicated by blue, $\beta$2 (51−54) by cyan, $\beta$3 (58−60) by ice-blue, and helix $3_{10}$ (79−84) by green. All eight cysteine residues are shown by licorice. The closest initial distances between the protein and the surface are also indicated.

Mutational studies on human lysozyme have indicated that Lys1, Arg10, Lys13, and Arg14 play an important role in protein binding to the hydroxyapatite surface.[43] Those residues correspond to Lys1, Lys13, and Arg14 in HEWL (with Arg10 replaced by Ala10) and are located on the N,C-terminal protein face,[44] again indicating side-on orientation on the surface. Results of fluorescently labeled (Cy5 dye) HEWL adsorption on chromatographic resins partially confirm this selection.[22] According to Dismer et al.,[22] HEWL possesses two adsorption binding sites; the first one consists of Lys1 and Lys33, and the second one contains Lys33 and Lys116. At low pH, the HEWL−surface binding mechanism is dominated by the first binding site, whereas the contribution of the second binding site increases with rising pH.[22] Residues Lys1, Lys13, and Arg14 are located at the side site of the HEWL molecule, close to the C-terminus (Lys129) and at the back of the active site, whereas

Lys33 and Lys116 are placed on the end-site of the molecule, close to the active site.[44] It has been found that the positively charged C-terminus might be attracted to the negatively charged surface.[32]

Atomic force microscopy (AFM) experiments have indicated that HEWL adsorbed on mica is still mobile.[27,29−31] Comparison of experimental images and Monte Carlo simulations shows that adsorbed proteins diffuse on the mica surface with a diffusion coefficient of $10^{-16}$ cm$^2$/s to form clusters, and that cluster diffusion is also evident.[29−31] The protein orientation on the surface appears to depend on the surface coverage; at low coverage, lysozyme preferentially adsorbs side-on, while the contribution of molecules adsorbed end-on increases with surface coverage.[30] This same approach also shows that HEWL adsorbs onto the bare mica surface with finite probability, possibly related to the protein orientation when next to the surface.[31] This result is reminiscent of other two-state adsorption models suggested in the literature.[19,42]

Despite recent theoretical and numerical investigations, including Brownian dynamics,[45,46] Monte Carlo simulations,[29−31,47] and numerous molecular dynamics (MD) studies for human lysozyme[48−51] and the HEWL protein,[31,52−55] atomistic details of lysozyme adsorption, cluster formation, and protein/cluster diffusion on the mica surface remain unknown. Here, we present results of systematic, fully atomistic MD simulations of HEWL. While we are limited to the initial events during the adsorption process, we can investigate the protein conformational changes upon adsorption in detail, identifying the time period in which conformational alteration takes place and the extent of the changes. We are also able to investigate whether electrostatics provides the dominant adsorption forces, the orientational dependence of adsorption, the key residues involved, the role of water layers at the surface, and the impact nonflat surfaces have on the denaturation of the protein. To the best of our knowledge, this is the first systematic MD modeling of lysozyme adsorption on a charged solid surface.

## Molecular Dynamics Protocol

We start with the X-ray structure of HEWL (PDB: 1iee) solved by Sauter et al.,[43] keeping all four disulfide bridges. All trajectories were performed using NAMD 2.6[56] with the Charmm27 forcefield; neutralization, solvation, and trajectory visualization were performed using VMD.[57]

We have prepared seven systems. Two systems contained one HEWL molecule placed in a rectangular box of water molecules (TIP3P) that extend 8 Å from any protein atom, as shown in Figure 1a. Since the net protein charge was +4e, the systems were neutralized by adding NaCl salt with ionic strengths of 0.5 M (mol/L) and 0.02 M; the number of atoms in both cases was about 15 000. 20 ns trajectories were treated as a reference for protein−surface systems with ionic strengths of 0.5 and 0.02 M, respectively.

Three other systems contained HEWL and a $SiO_2$ surface (mimicking a mica surface) located in three different orientations with respect to the protein (see Figure 1b−d). In the case of orientation 1, we have used ionic strengths of 0.5 and 0.02 M, while, in the case of orientations 2 and 3, one ionic strength (0.02 M) was used. The surface 86.4 Å × 92.8 Å was built from a square array of silicon and oxygen atoms located 1.6 Å away from each other with charges of +1.11e and −0.66e, respectively. Surface atoms were fixed in all stages of the MD simulations. The resultant surface charge density of $\sigma = -0.0217$ e/Å$^2$ is almost equal to that of mica at pH 7 ($\sigma = -0.021$ e/Å$^2$); see ref 47. Such parameters allowed us to use a single $SiO_2$ plane surface to simulate the mica surface. Neutralized protein was placed close to the surface, and then, the whole HEWL−surface system was solvated in a water box that extends at least 20 Å from any protein atom and 1 Å from any surface atom. Since in all studied protein−surface systems the neutralized protein and the charged surface were put together, the net charge was equal to the surface charge. As is shown in Figure 1b, in the case of orientation 1, the surface was located about 8 Å away from the closest HEWL side chain (Arg128) and about 12 Å away from the protein backbone (Arg128). In the case of orientation 2 (Figure 1c), the surface was located about 7 Å away from the closest HEWL side chain (Arg112) and about 10 Å away from the protein backbone (Asp48). In orientation 3, the initial protein−surface distance was 9.59 Å (Figure 1d). In the simulations, the distances between residues and the plane of the surface were monitored to identify adsorption events and the residues involved. The HEWL−surface system after solvation contained about 51 000 atoms, and the number of atoms was not dependent on the protein−surface orientation.

The last system (HEWL−cage system) was built from HEWL placed in the center of a rectangular box with dimensions of 86.4 Å × 92.8 Å × 89.6 Å (for an illustration, see Figure 1e and Supporting Information Figure S1). The closest distances between HEWL side chains and every cage wall were 22.5 Å (Arg128), 23.2 Å (Asn19), 23.7 Å (Arg45), 27.2 Å (Arg73), 27.3 Å (Arg112), 27.5 Å (Arg125), and 29.7 Å (again Arg128, distance to the other wall). The cage was filled by water, so the water box extended at least 22 Å from any protein atom. The HEWL−cage system containing about 72 000 atoms was not neutral as well, but the protein was neutralized as usual by adding NaCl salt in 0.02 M concentration. The Debye length ($r_D$) for ionic strengths of 0.5 and 0.02 M was about 22 and 61 Å, respectively.

Summarizing, the seven prepared systems (and trajectories) were as follows: (1) isolated HEWL with an ionic strength of 0.5 M; (2) isolated HEWL with an ionic strength of 0.02 M; (3) HEWL−surface system in orientation 1 with an ionic strength of 0.5 M; (4) HEWL−surface system in orientation 1 with an ionic strength of 0.02 M; (5) HEWL−surface system in orientation 2 with an ionic strength of 0.02 M; (6) HEWL−surface system in orientation 3 with an ionic strength 0.02 M; and (7) HEWL−cage system with an ionic strength of 0.02 M.

All systems were subject to 100 ps water equilibration, 10 000 steps of whole system minimization, 30 ps heating to 300 K, and 270 ps equilibration at this temperature. The production MD simulations were pursued for 20 ns at 300 K in the NVT ensemble. The integration step was 2 fs, and the SHAKE algorithm and PBC were used. The cutoff distance for both van der Waals and Coulomb interactions was 12 Å. For ionizable residues, the most probable charge states at pH 7 were chosen. We have no evidence of artificial build-up of momentum in the simulations, and no additional restrictions on momentum were used. In the case of the HEWL−surface system in orientations 1 and 2 (ionic strength 0.02 M), an additional 30 ns of trajectories were calculated; nevertheless, just the first 20 ns were carefully analyzed. Given the values of screening length $r_D$ in our simulations, we check the accuracy of cutoffs used for the nonbonding interactions. We have run test calculations for the HEWL−surface system in orientation 1 (ionic strength 0.02 M) using cutoffs of 24 Å and also the smooth particle mesh Ewald (SPME) summation (20 ns),[58] which neutralizes the cell charge by imposing a background jellium.[59] Because

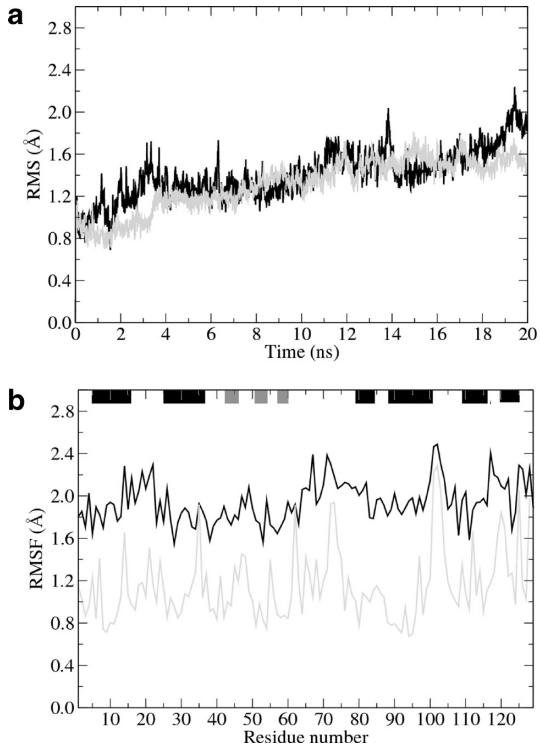


**Figure 2.** (a) The root mean square distance and (b) the root mean square fluctuations calculated with respect to the crystal structure. Results obtained from the trajectory for isolated HEWL protein with an ionic strength of 0.5 M (the black line) and 0.02 M (the gray line). The inset indicates secondary structure elements where α-helices are represented by black rectangles, $\beta$-structures by gray rectangles, and other structures like loops, hydrogen-bonded turns, and residues in isolated $\beta$-bridges by white rectangles.

of its very high computational cost, the trajectory with 24 Å cutoffs has been stopped after 500 ps.

## Results

**The Isolated HEWL Protein with Ionic Strengths of 0.5 and 0.02 M.** The 20 ns trajectories of solvated HEWL protein with 0.5 and 0.02 M ionic strength were treated as a reference for HEWL−surface systems. The dynamics of isolated proteins seems to not be affected much by the solute ionic strength. The root mean square (rms) distances with respect to the initial structure were calculated for both systems. Plots of rms distance vs time had similar, almost horizontal character and did not exceed a value of 2 Å (see Figure 2a). The long-term rms oscillations most likely were connected with opening and closing of the active site cleft (data not shown). The structural alternations of the protein were limited mainly to the loops; the secondary structure elements were well maintained. This is confirmed by root mean square fluctuation (rmsf) analysis (Figure 2b). It means that in both cases the loop regions were working as hinges connecting rigid secondary structure elements. Further illustration of extensive loop motion is provided by Figure 3a and Supporting Information S2A. Excluding normal fluctuations, the N- and C-terminus remained at the protein surface.

Information about changes in protein shape during the dynamics and/or adsorption process comes from analysis of the principal ellipsoid axes which are 45, 30, and 30 Å long.[20] As shown in Figure 4, the length of the axes can change during the protein dynamics. The slightly different initial values were probably caused by the different definitions of the axes in

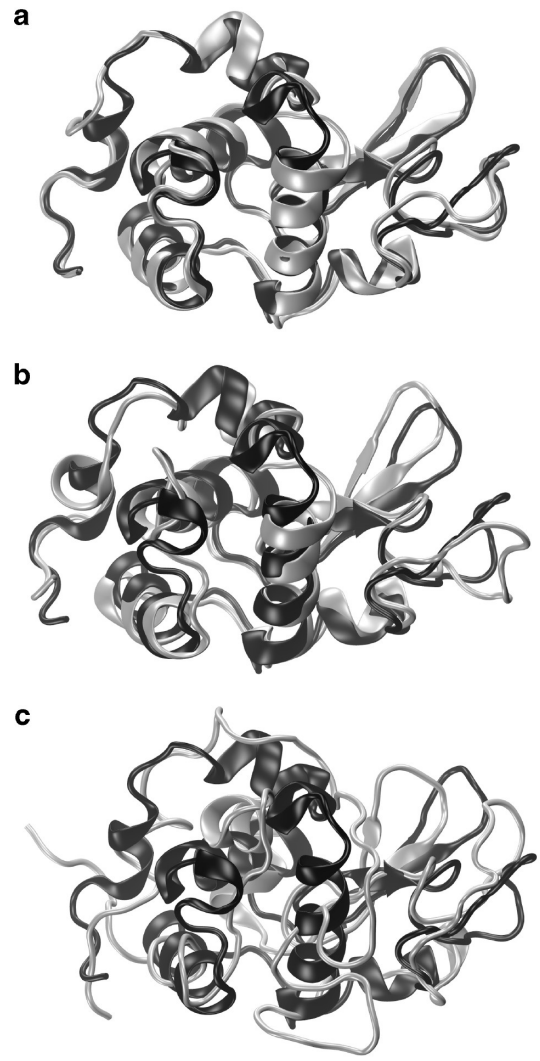


**Figure 3.** The superposition of initial (black) and final (gray) structures of (a) the isolated HEWL protein with an ionic strength of 0.02M, (b) the HEWL−surface system in orientation 1 with an ionic strength of 0.02 M, and (c) the HEWL−cage system. Just the protein backbone is shown.

experiment and our simulations. In the system with an ionic strength of 0.5 M, the length of the major axis was fluctuating around a value of 42 Å, whereas, in the system with a 0.02 M ionic strength, the axis length slowly decreased from ∼43 to ∼41 Å. The length of the minor one rapidly decreased at about 3 ns from ∼31 to ∼27 Å, and then was again relatively stable. This observation was independent of the solute ionic strength.

**HEWL−Surface System with an Ionic Strength of 0.5 M in Orientation 1.** As is shown on Figure 5a, during the whole 20 ns trajectory of the HEWL−surface system with a 0.5 M ionic strength, the rms (calculated with respect to the initial structure) did not exceed a value of 2 Å and at the final stages of the trajectory was fluctuating around 1.8 Å. Fluctuations again seem to be connected with the opening and closing of the active site cleft (data not shown). Comparison with results obtained for the isolated HEWL system with the same ionic strength, excluding the 15−18 ns period, showed that presence of the surface induced rather small (if any) alternations in protein structure. The disagreement in rms shape in the 15−18 ns period is connected with a change of protein orientation with respect to the surface (see below). The average rms value for the whole trajectory was 1.50 and 1.41 Å for the HEWL−surface and the isolated protein, respectively.

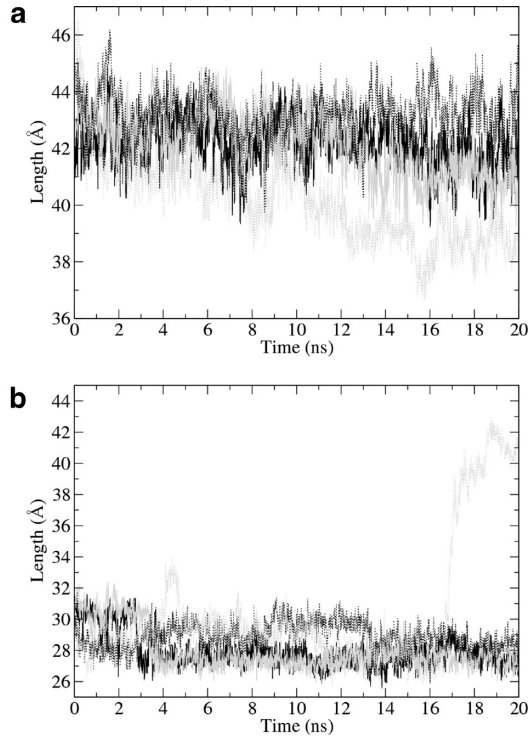


**Figure 4.** Length of the principal axes of the HEWL ellipsoid in 20 trajectory of isolated HEWL protein with an ionic strength of 0.5 M (the black line) and 0.02 M (the gray line), the HEWL−surface system in orientation 1 (the black dotted line), and the HEWL−cage system (the gray dotted line): (a) the major axis; (b) the minor axis.

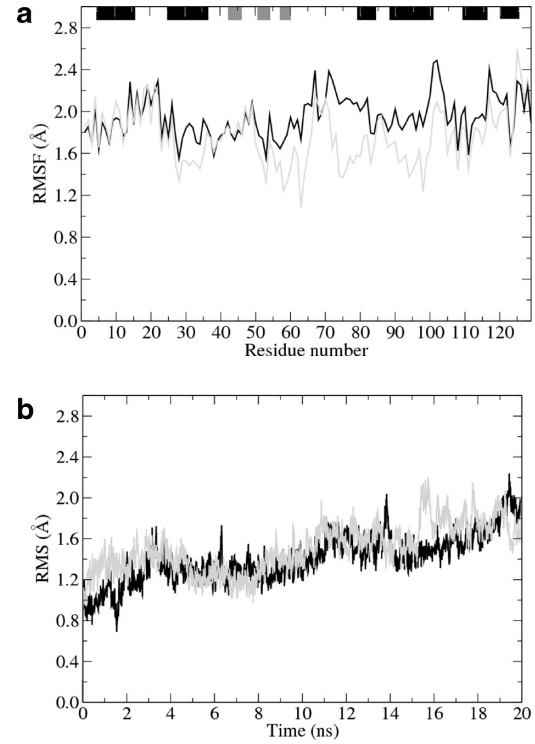


**Figure 5.** (a) rms and (b) rmsf plots obtained for the isolated HEWL protein with an ionic strength of 0.5 M (the black line) and the HEWL−surface system with an ionic strength of 0.5 M (the gray line). The inset indicates secondary structure elements where α-helices are represented by black rectangles, $\beta$-structures by gray rectangles, and other structures like loops, hydrogen-bonded turns, and residues in isolated $\beta$-bridges by white rectangles.

The rms values calculated separately for the secondary structure elements shown in Figure 1—α-helix A (residues 5−16), α-helix B (25−37), α-helix D (109−116), α-helix $3_{10}$ from domain α (120−125), α-helix $3_{10}$ from domain $\beta$ (79−84), B1 $\beta$-sheet (43−46), and B2 $\beta$-sheet (41−54)—were not higher than 0.5 Å. In the case of α-helix C (residues 88−101) and B3 $\beta$-sheet (58−60), the rms reached a value of 1 Å. The biggest contribution to the rms came from the loops. Almost identical results were obtained in the case of isolated HEWL protein with 0.5 M ionic strength.

Residue fluctuations (rmsf's) are usually treated as a second indicator of the trajectory quality. As is shown in Figure 5b, the fluctuations did not exceed a value of 2.2 and 2.4 Å in the HEWL−surface and isolated protein, respectively. The average fluctuations (for the whole protein) were 1.85 and 1.96 Å. The fluctuation maxima, in both trajectories, were observed for residues 65−78 and 100−105. Residues 65−78 are a part of the longest loop, and the sodium ion binding site is located in this region. The loop 100−105 links two α-helices: C and D. The average fluctuations at the secondary structure elements were 1.67 and 1.87 Å for the HEWL−surface and the isolated protein, respectively, which implies that the secondary structure was well maintained in both trajectories.

During the first 10 ns of dynamics, the protein moves away from the surface. Simultaneously, the conformation of loops, especially the long loop 68−75, changes and thus the orientation of the secondary structure elements with respect to each other alters slightly too (for illustration, see Supporting Information Figure S2B). Following this, the protein starts to slowly translate toward the surface. Between 14 and 18 ns, this movement is accompanied by a slow rotation. During the last 2 ns, the adsorption rate is slightly enhanced. As indicated in Table 1, the most crucial residue for the protein−surface interaction is Arg128. A possible role for Arg14 is also not excluded.

**TABLE 1: The Smallest Distances between Protein and the Silica Surface Observed in the Initial and Final (after 20 ns of Dynamics) Structures Obtained for the HEWL−Surface System in Orientation 1 with an Ionic Strength of 0.5 M**

| | distance (Å) | |
|---|---|---|
| protein residue | initial | final |
| Lys1 | 10.48 | 22.21 |
| Arg5 | 18.30 | 14.31 |
| Arg14 | 10.46 | 8.81 |
| Arg128 | 7.89 | 4.66 |

Examination of the principal HEWL ellipsoid axes as well as the solvent accessible area of individual residues (data not shown) indicates that the protein shape is not significantly changed in these dynamics and the early events of adsorption.

**HEWL−Surface System with an Ionic Strength of 0.02 M in Orientation 1.** Analysis of the rms calculated with respect to the initial structure showed that in the case of systems with an ionic strength of 0.02 M the presence of the surface influenced the protein dynamics. As shown in Figure 6a, the rms calculated for this HEWL−surface system was always about 1 Å higher that those calculated for the isolated HEWL protein with the same (0.02 M) ionic strength. In both cases, the rms reached equilibrium, but the long-term rms oscillation amplitude was also higher in the trajectory with the surface than without. The average rms value calculated over the 20 ns trajectory period was equal to 2.26 and 1.31 Å for the HEWL−surface and isolated HEWL systems, respectively. rms values were also calculated separately for each secondary structure element. The character of the rms plots obtained for the structures α-helix A, α-helix B, α-helix C, α-helix $3_{10}$ from the $\beta$-domain, and $\beta$-sheets B1 and B2 were small and similar to the isolated

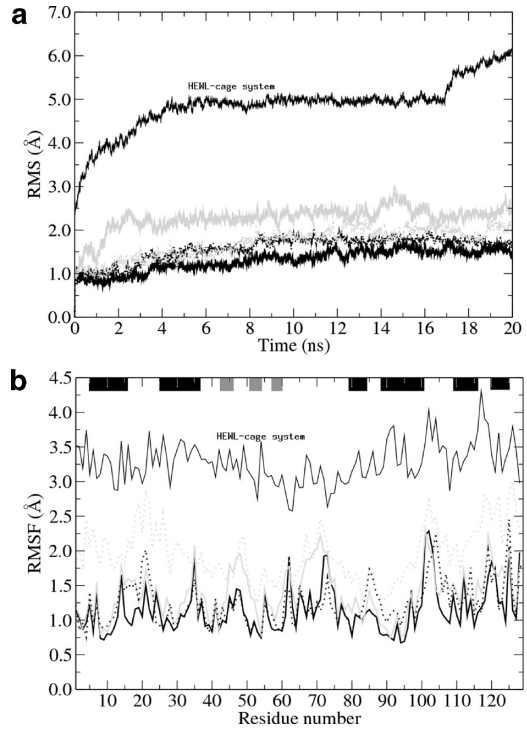


**Figure 6.** (a) rms and (b) rmsf plots obtained for the isolated HEWL molecule (the black line), the HEWL−surface system in orientation 1 (the gray line), the HEWL−surface system in orientation 2 (the black dotted line), the HEWL−surface system in orientation 3 (the gray dotted line), and the HEWL−cage system (the labeled line). The ionic strength was always 0.02 M. The inset indicates secondary structure elements where α-helices are represented by black rectangles, $\beta$-structures by gray rectangles, and other structures like loops, hydrogen-bonded turns, and residues in isolated $\beta$-bridges by white rectangles.

HEWL system. In the case of the structures α-helix D, α-helix $3_{10}$ from the α-domain, and $\beta$-sheet B3, the plot shapes were comparable in both trajectories (with and without the surface), but the numbers were always a little higher in the HEWL−surface system. This suggests that the presence of the surface may destabilize these three structures. Nevertheless, the main contribution to rms comes from the loop regions. This observation is supported by Figure 3b; after 20 ns of trajectory, changes in the relative orientation of secondary structure elements and partial loss of the α-helix content are clearly visible. The location of the C-terminus also differs between initial and final structure. The average rmsf's for the trajectory are similarly higher than for the isolated HEWL.

The average rms values calculated from the trajectory with and without the surface for the secondary structure elements were 1.30 and 1.06 Å, at the loop regions were 1.45 and 1.20 Å, and for the whole protein were 1.39 and 1.15 Å, respectively. The maximal values were observed at the 66−74 and 101−103 regions (loops).

In this system, the protein started to move toward the surface from the beginning of the trajectory. This movement was accompanied by small rotations and translations in the plane parallel to the surface (data not shown). As listed in Table 2, the initial distance between the protein and the surface was about 7 Å and the final less than 2 Å. Attraction between the HEWL and the surface was visible after about 3.5 ns of the trajectory. At this moment, the side chains of Arg14 and Arg128, initially parallel to the surface, reached a perpendicular orientation with respect to the surface (data not shown). As is indicated in Table 2, Lys1 and Arg5 may also be important for HEWL−surface

**TABLE 2: The Smallest Distances between Amino Acids and the Silica Surface in the Initial and Final (after 20 ns of Dynamics) Structures Obtained for the HEWL−Surface System in Orientation 1 with an Ionic Strength of 0.02 M**

| | distance (Å) | |
|---|---|---|
| protein residue | initial | final |
| Lys1 | 10.48 | 4.18 |
| Arg5 | 18.30 | 2.96 |
| Arg14 | 10.46 | 7.00 |
| Arg128 | 7.89 | 1.93 |

interactions. Since in the initial structure Arg5 was pretty far from the surface, this residue was not labeled in Figure 1b. Graphical analysis suggested that conformational changes, at least in the α-helix $3_{10}$ from domain α and the long 61−75 loop, were required for adsorption. Conformational alterations were accompanied with changes in the relative orientation of secondary structure elements (Figure 3b) and protein shape as well.

As is shown in Figure 4, the major HEWL ellipsoid axis was fluctuating around a value of ∼43.5 Å, while in the isolated HEWL protein its length decreased from ∼43.5 to ∼41.0 Å. The length of the minor axis at the end of the trajectory reached the same value as in the system without the surface; nevertheless, its evolution was different in the two systems. The final angle between the major axis and the surface was about 45° and the N,C-terminal face was turned toward the surface.

The HEWL motion toward the surface disturbed the highly organized, structured water layers on the surface. The side chains of Lys1 and Arg14 perturbed only the outer water layer, whereas the Arg128 side chain thrust through the outer and inner layer. The side chains were interacting with the surface mainly via water molecules; nevertheless, direct interactions were also observed. An extended hydrogen-bond network between the penetrating side chain and the water layers was always observed.

An additional 50 ns trajectory did not show any new features. The role of Lys1 and Arg5 for protein−surface interactions was confirmed and two new residues interacting with the surface, Val2 and Glu7, were found (data not shown). Protein diffusion on the surface was not detected, as expected since the HEWL diffusion coefficient on the mica surface is $10^{-16}$ cm$^2$/s.[29−31]

The overall trends observed for this system were independent of the calculation method for the nonbonding interactions. In the 20 ns trajectory using the SPME method, the protein structure was not much different, only displaying a slightly enhanced loss of the α-helix content (for details, see Supporting Information Figure S2C). The selection of the important residues for the protein−surface interactions (Lys1, Val2, Arg5, Glu7, Arg125, and Arg128) was almost the same as in the standard trajectory. The protein motion toward the surface and its final shape and orientation all had the same character as in the standard simulation. The water dynamics on the surface was also not affected by the calculation method (data not shown). A similar conclusion is drawn from the short 0.5 ns trajectory with the 24 Å nonbonding interaction cutoff.

**HEWL−Surface System with an Ionic Strength of 0.02 M in Orientation 2.** The rms calculated for the HEWL−surface system in orientation 2, shown in Figure 6a, was almost identical to that calculated for the isolated protein with the same ionic strength, indicating that the protein conformation was kept (average 1.58 Å, maximal 1.80 Å). In the case of isolated protein, the average and maximal rms values were 1.31 and 1.50 Å, respectively. This 0.2−0.3 Å difference also suggests that the surface placed opposite to the N,C-terminal part of the

**TABLE 3: The Smallest Distances between Amino Acids and the Silica Surface in the Initial and Final (after 20 ns of Dynamics) Structures Obtained for the HEWL−Surface System in Orientation 2 with an Ionic Strength of 0.02 M**

| | distance (Å) | |
|---|---|---|
| protein residue | initial | final |
| Thr47 | 8.13 | 16.18 |
| Asp48 | 9.19 | 16.08 |
| Asn103 | 8.57 | 15.03 |
| Arg112 | 7.29 | 15.86 |
| Lys116 | 9.09 | 15.14 |

HEWL surface does not have a significant influence on the protein structure and conformation. rms distances calculated separately for secondary structure elements were also very similar to those obtained in the case of isolated protein.

The same picture emerges from the rmsf plot (Figure 6b). The average fluctuations for the whole protein, secondary structure elements only, and loop regions only were 1.25, 1.14, and 1.34 Å, respectively. This means that protein secondary structure elements, as well as loop conformation, were maintained. Supporting Information Figure S2D supports this observation. Apart from the loop regions, the main difference between the initial and final orientation was seen in the case of α-helix $3_{10}$ from domain α (residues 120−125), which rotated around the loop 117−119. Slight differences between rms and rmsf plot shapes obtained for the isolated protein and the HEWL−surface system in orientation 2 reflect different statistics rather than different protein behavior. Evolution of the principal HEWL ellipsoid axis (data not shown) supports this interpretation.

During this simulation, the protein moved away from the surface, as Table 3 indicates. The closest distance between the protein and the surface was about 7.3 Å (Arg112) at the beginning and about 15 Å after 20 ns of dynamics. It is worth noting that the list of the closest residues includes Lys116. During an additional 30 ns trajectory, the protein started to strongly interact with the image of the surface, the main interacting residues being Arg128, Lys1, and probably Glu7 (data not shown). This was accompanied by slight conformational changes similar to those observed for the system in orientation 1 (data not shown).

**HEWL−Surface System with an Ionic Strength of 0.02 M in Orientation 3.** The rms calculated for the HEWL−surface system in orientation 3, shown in Figure 6a, initially grows for 10 ns and then reaches a plateau at ∼2 Å. Longer-time oscillations were higher than those in orientation 2; nevertheless, the rms values were usually somewhere between those obtained in orientations 1 and 2. Analysis of the rms calculated separately for secondary structure elements (data not shown) shows that the main contribution comes from the loop regions. Moreover, similar to the results for orientation 1, it indicates that the structures α-helix D, α-helix $3_{10}$ from the α-domain, and $\beta$-sheet B3 are relatively unstable (rms ∼0.5 Å or more) and more flexible than in the previous systems. This observation is confirmed by the rmsf shown in Figure 6b; fluctuations in orientation 3 are always higher than in orientation 1 or 2. However, all mobile secondary structure elements are far away from the unfolded state (see also Supporting Information Figure 2SE) and the maxima occur at the loops. Altogether, this suggests that the surface located in orientation 3 with respect to the protein induces noticeable protein destabilization but without secondary and tertiary structure reorganization.

In this system, the surface induces significant protein rotation alongside small movement toward the surface. As shown in Figure 1d and Table 4, the initial protein−surface distance was ∼9.5 Å, while the final was ∼2 Å. Graphical analysis indicated that distance decrease is caused more by rotation than translation. During the 20 ns period, the HEWL rotated ∼42° with respect to the initial protein−surface orientation, to align the N,C-terminal face. Initially, the angle between the HEWL ellipsoid major axis and the surface was about 45°; the same angle measured from the N,C-terminal protein face was obtuse (135°). After 20 ns, the angle was almost equal to 90° and the C-terminus reached the location close to the surface. It is possible that at longer time scale the protein rotation would be continued until the angle measured from the N,C-terminal face is ∼45° with the face turned toward the surface. The most important residues for protein−surface interactions are Arg128 and Arg125. A significant role for the N-terminal Lys1 and Arg5 is also not excluded, since they came closer to the surface by 10 Å (Table 4).

**TABLE 4: The Smallest Distances between Amino Acids and the Silica Surface in the Initial and Final (after 20 ns of Dynamics) Structures Obtained for the HEWL−Surface System in Orientation 3 with an Ionic Strength of 0.02 M**

| | distance (Å) | |
|---|---|---|
| protein residue | initial | final |
| Lys1 | 29.66 | 20.74 |
| Arg5 | 19.20 | 9.55 |
| Arg14 | 17.66 | 15.13 |
| Asn19 | 10.70 | 18.26 |
| Gln121 | 10.16 | 8.77 |
| Arg125 | 15.06 | 4.16 |
| Arg128 | 9.59 | 2.38 |

**HEWL−Cage System.** In the case of the HEWL−cage system with an ionic strength of 0.02 M, the rms (Figure 6a) strongly suggests the protein has lost its structure. The high slope of the rms curve observed in the first 4 ns indicates that the main conformational changes have taken place during early stages of the dynamics. From 4 ns until 17 ns, the rms had a horizontal character with a value of ∼5 Å, which means that the protein achieved a stable, partially unfolded intermediate structure. At ∼17 ns, the next conformational change has taken place and the rms suddenly jumped to ∼5.5 Å, followed by a steady increase. At this point, the N-terminus detached from the protein surface and started to strongly interact with the silica surface. Within 0.25 ns, the distance between its closest neighbors, Thr40 and Ala42, increased from 5.5 and 11.5 Å to 21 and 24 Å, respectively. The distance from its starting position increased from 4 Å at 17 ns to 24 Å at 18 ns. In the same time period, the distance between Lys1(Cα) and the closest cage wall decreased from 29 to 8 Å, and the Lys1 side chain came from 28 to 6 Å. This rapid orientation change of the N-terminus initialized the unfolding of the α-helix A (residues 5−16). The subsequent slow growth of the rms reflects continuing protein unfolding. The position change of the N-terminus is visible in Figure 3c, and further details are given in Supporting Information Figure S3.

As shown in Figure 6b, fluctuations were relatively high, usually >3 Å, suggesting that the protein secondary structure was lost. Analysis of the rms calculated separately for all secondary structure elements, as well as graphical analysis, indicated that during the first 4 ns α-helix C (residues 33−101), α-helix D (residues 109−116), and α-helix $3_{10}$ from domain α (residues 120−125) were unfolded. α-helix B (residues 25−37) was bent rather than unfolded. $\beta$-structure B3 was unfolded during the heating and equilibration stages (the preparation period). α-helix $3_{10}$ from domain $\beta$ (residues 79−84) was slowly

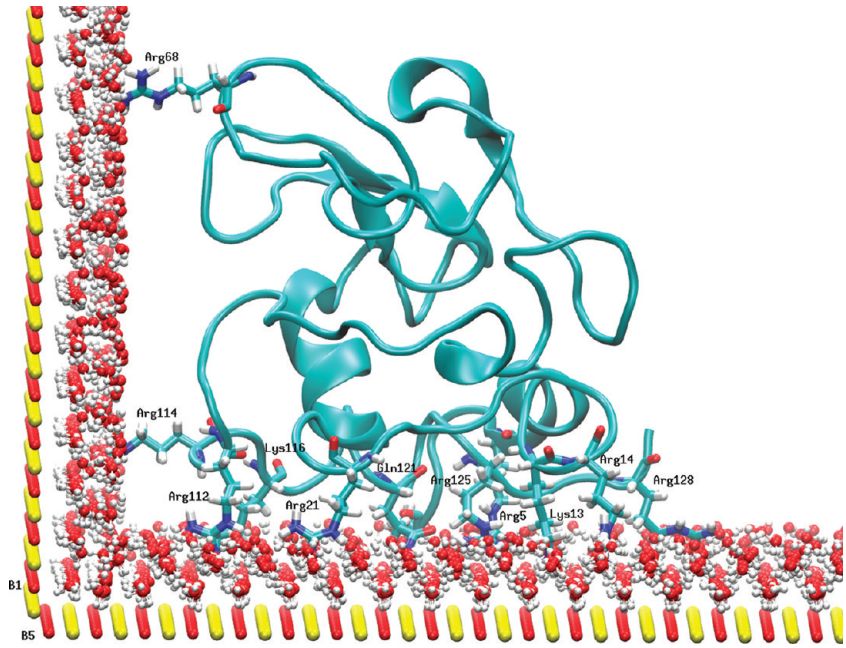


**Figure 7.** The HEWL−cage system after 20 ns of trajectory. Two important walls of the cage, B1 and B5, as well as two structured water layers are shown by CPKs. The protein is shown as a cartoon, and the most important residues interacting with the silica surface are shown by licorice and labeled.

unfolding between 4 and 17 ns but did not reach a totally unfolded state. As mentioned above, α-helix A started to unfold after 17 ns of dynamics; this process was continued until the end of the trajectory. $\beta$-structures B1 (residues 43−46) and B2 (residues 51−54) were the only two totally intact secondary structure elements. The huge conformational changes observed in the dynamics can be visualized in Figure 3c.

As mentioned above in the MD protocol section, the HEWL was initially located in the center of the cage. Distances between the surface residues and the cage walls varied from 22.5 to 29.7 Å, depending on the cage wall (see also Figure 1e and Supporting Information Figure S1). In the dynamics, the protein immediately came to the cage walls. After 1 ns of the trajectory, Arg14, Arg21, Lys116, Arg125, and Arg128 were only 6 Å away from the cage wall B5, while Arg114 was 6 Å away from the wall B1. After about 10 ns, at least six residues—Arg14, Arg112, Arg114, Lys116, Gln121, and Arg125—were 4.5−5 Å away from one of the walls (B1 or B5) and this distance was subsequently stable over time. Residues Arg5, Lys13, Arg21, Arg68, and Arg128 were also close to the surface after this period (data not shown). The last event we observed in the adsorption process occurred after 19 ns of the dynamics, and it was related to the change of the N-terminus conformation (see Supporting Information Figure S3). The distance between Lys1 and the wall B5 has decreased from ∼30 to ∼4.5 Å at the end of the trajectory. Among the mentioned residues, only Arg68 and Arg114 were interacting with wall B1; others located on the N,C-terminal part of the HEWL surface were attracted by wall B5 (see Figure 7). The closest distances between the side chains and the cage atoms at the beginning and at the end of the trajectory are listed in Table 5. It is worth noting that sometimes the closest surface atom to the given residue at the beginning belongs to the different wall than at the end.

Molecules from the structured water layers at the cage surfaces were pushed out from the outer layer by various side chains. The inner water layer was not affected; the protein penetrated only the outer layer. As shown in Figure 7 and Supporting Information Figure S4, the adsorbed protein shape was very different from the shape of the free protein.

The evolution of the principal HEWL ellipsoid axes in the HEWL−cage system is shown in Figure 4, alongside those from the isolated protein and HEWL−surface system in orientation 1. The major axis slowly decreased from ∼46.0 to ∼39.0 Å. This behavior was quite similar to the isolated protein (decrease from about 43.5 to 41.0 Å). The huge difference was found in the case of the minor axis, where at about 16.5 ns its length increased from ∼27 to ∼42 Å. This change correlates well with the conformational change of the N-terminus (see Supporting Information Figure S3).

## Discussion

**Conformational Stability upon Adsorption on the Flat Surface.** Comparison of the trajectory obtained for the HEWL−surface system with that obtained for the isolated protein with the same 0.5 M ionic strength shows that the overall dynamical features such as protein flexibility, including the mobility of the loops in general, have the same character. The good agreement in rmsf values obtained for the isolated and HEWL−surface system indicate that, in the high salt concentration, the presence of the surface does not strongly influence the protein structure and dynamical behavior. This observation is supported by rms distances and graphical analysis.

The rms and rmsf values for the protein−surface system in orientation 1 with an ionic strength of 0.02 M imply that, contrary to the system with high salt concentration, the presence of the surface induces changes in the relative orientation of secondary structure elements and conformational alteration in three structures: α-helix D, α-helix $3_{10}$ from α-domain, and $\beta$-sheet B3. More intense loop movement and the rmsf maxima found in the region 61−75, which is a part of a long, flexible loop that is also quite mobile in the crystal structure,[43] suggest that the protein is more flexible when the surface is present and the salt concentration is small (0.02 M). This result agrees with previous experimental observations that the adsorbing protein adopts a more flexible structure.[40] Bending of the 61−75 loop probably enables the protein to adopt a lower energy conformation on the surface. Visually, it appears that the above-

**TABLE 5: The Smallest Distances between Amino Acids and the Silica Surface in the Initial and Final (after 20 ns of Dynamics) Structures Obtained for the HEWL−Cage System**

| | | distance to the closest atom (Å) | |
|---|---|---|---|
| protein atom | the closest wall | initial | final |
| The Smallest Distances at the Beginning of the Trajectory | | | |
| Asn19(Hδ21) | B5 | 23.21 | 11.44 |
| Arg45(HH21) | B6 | 23.76 | 9.67 |
| Arg73(HH22) | B3 | 27.17 | 17.25 |
| Arg112(HH11) | B1 | 27.30 | 4.02 |
| Arg125(Hε) | B2 | 27.30 | 4.00 |
| Arg128(HH21) | B5 | 22.53 | 4.09 |
| Arg128(HH22) | B4 | 29.72 | 5.03 |
| The Smallest Distances at the End of the Trajectory | | | |
| Lys1(Hζ3) | B4 → B5 | 31.47 | 3.52 |
| Arg5(HH22) | B2 → B5 | 30.19 | 4.28 |
| Lys13(Hζ2) | B5 | 24.66 | 4.09 |
| Arg14(HH22) | B5 | 30.64 | 3.90 |
| Arg21(HH22) | B5 | 27.54 | 4.01 |
| Arg68(HH21) | B6 → B1 | 24.07 | 6.00 |
| Arg112(HH21) | B1 → B5 | 27.29 | 4.02 |
| Arg114(HH21) | B2 → B1 | 31.72 | 4.25 |
| Lys116(Hζ3) | B1 → B5 | 29.07 | 3.49 |
| Gln121(Hε22) | B5 | 23.17 | 4.49 |
| Arg125(HH21) | B2 → B5 | 27.49 | 4.00 |
| Arg128(HH12) | B5 | 22.53 | 4.22 |

mentioned α-helices are starting to unfold. The loss of the α-helix content upon HEWL adsorption is also observed experimentally.[6,39] Nevertheless, alterations were rather marginal and after 20 ns all of these structures were far from the unfolded state.

The silica surface initially located opposite the N,C-terminal part of the protein (system in orientation 2) does not strongly alter the protein structure and dynamical behavior. The rms and rmsf values were just slightly higher than in the case of the isolated system with the same, 0.02 M, ionic strength. Protein secondary and tertiary structure was well maintained during the 20 ns trajectory, and the loop dynamics were almost identical to those in the isolated protein. The situation slightly changed in the late stages of the dynamics, and during the additional 30 ns trajectory, when the protein started to strongly interact with the surface image. That stage imitated the protein behavior observed in the orientation 1 system.

In the case of orientation 3, the surface induced more pronounced tertiary protein structural alternations than in orientation 1, mediated through the loop region motions. However, despite the high flexibility, all the secondary structure elements were quite well maintained, even more so than in orientation 1, and the protein had adopted an optimal adsorption structure and orientation with respect to the surface. Notwithstanding the small loss of the α-helix content (α-helix D, α-helix $3_{10}$ from α-domain) and problems with $\beta$-sheet B3, the protein secondary structure was not changed much and unfolding was not observed.

**Adsorption Driving Force.** In the second half of the trajectory calculated for the HEWL−surface system in orientation 1 with 0.5 M ionic strength, a weak attraction between protein and the silica surface was observed. Despite its lower intensity, the overall trends and list of the most important residues was consistent with results obtained in the case of the protein−surface system in orientation 1 with an ionic strength of 0.02 M. The most likely explanation of slow protein movement toward the surface is strong screening of the electrostatic interactions which constrained the protein attraction to the surface. During the first 18 ns, the protein orientation changed, after which the attraction between the HEWL and the surface started to be visible. The slow rate of HEWL positioning, as well as a small number of side chains directly attracted to the surface (Arg14 and Arg128), suggests that the screening of electrostatic interactions was very effective at 0.5 M ionic strength. Low ionic strength causes enhancement of the adsorption process. Such a result agrees with numerous experimental data which suggest that adsorption is sensitive to the solvent ionic strength and in high salt concentrations is not effective.[5,11,17,21,31] Metropolis Monte Carlo studies have also showed that adsorption is increased by decreasing salt concentration.[47] Since a solvent ionic strength higher than 0.5 M prevents adsorption,[32] the observed slowdown of adsorption in 0.5 M ionic strength with respect to 0.02 M is perfectly reasonable. The trajectory obtained for the HEWL−surface system with 0.5 M ionic strength afforded better insight into the early events of adsorption.

As mentioned above, in the case of the HEWL−surface system in orientation 1 with an ionic strength of 0.02 M, the protein attraction by the surface was clearly visible. The protein adsorption was facilitated by its translations and rotations with respect to the surface. Translations were continued even when the protein can be considered as adsorbed (distance to the surface of ∼3 Å). Chemical bonds were not observed between the protein and the surface, the shortest observed distance being ∼2 Å, implying high electrostatic interaction energy. The list of the closest residues is consistent but more extensive than in the case of the HEWL−surface system at an ionic strength of 0.5 M. It is worth noting that the positively charged arginine residues detected in orientation 1 were also important in the case of orientation 3.

Analysis of the protein dipole moment orientation with respect to the surface supports the hypothesis that electrostatics governs the adsorption. The protein dipole moment was always oriented approximately from the active site cleft to the N,C-terminal protein face, and this internal direction did not depend on the ionic strength nor the silica surface orientation with respect to the protein. In all trajectories obtained for HEWL−surface systems, the value of the dipole moment was slightly fluctuated around the initial value (∼160 D). In the case of systems in orientation 1, the dipole moment was oriented toward the surface; in the system in orientation 2, it was against the surface and toward its image. In the case of the HEWL−surface system in orientation 3, the angle between the dipole moment and the surface changed from about 20° at the beginning of the trajectory to about 60° at the end. All of this together implies that the electrostatic interactions are the main force governing monolayer adsorption and hydrophobic/hydrophilic forces may work at most as supplementary forces. The importance of electrostatic interactions for HEWL adsorption was found in previous Brownian dynamics studies.[45,46] However, the driving force for second and further protein layer formation in multilayer adsorption may involve hydrophobic or hydrophilic interactions between protein layers.

The dominant role of electrostatics necessitates further consideration of the simulation methodology. The NAMD simulations are efficient with a fairly short nonbonding interaction cutoff of 12 Å. However, the Debye screening length is longer than this even in the 0.5 M solution. For this reason, we ran test simulations of the HEWL−surface in orientation 1 using both the SPME[58] summation and a longer 24 Å cutoff. In the former, the long-range electric field due to the net surface charge is suppressed using a background jellium model,[59] so that only

short-range effects close to the surface will be felt, replicating aspects of the cutoff methodology. As already discussed, no substantial differences are observed during this simulation. Using the longer cutoff distance, which substantially slows down the simulation and restricts us to a shorter run time of 500 ps, we again find no substantial effect on the trajectory. We conclude that the simulations we present here can give a good account of the close-range interactions between the protein and the surface. Longer-range effects, such as the rotation of the protein to align with the surface electric field within the Debye screening length, cannot be detected in these simulations.

**Protein Orientation on the Flat Surface.** As mentioned above, the protein orientation on the surface was forced by the dipole moment direction. Hence, the most important residues for adsorption, as hypothesized in previous experimental studies,[22,32] should be situated on the N,C-terminal protein face. In fact, residues detected in the case of trajectories obtained for HEWL−surface systems with ionic strengths of 0.5 M (Arg14 and Arg128) and 0.02 M (Lys1, Arg5, Arg14, and Arg128) are part of the N,C-terminal protein surface. This is also true for the HEWL−surface system in orientation 3 (residues Arg125 and Arg128). The location and list of important residues is consistent with the previous experimental list[43] and the main adsorption site found experimentally by Dismer et al.[22]

The trajectory for the HEWL−surface system in orientation 2 provides further support of the idea that the N,C-terminal protein face is a preferential site for adsorption on the flat surface. In this case, the initial protein−surface distance was about 7 Å (see Figure 1c), the protein−image of the surface distance was about 13 Å, and the protein size in this direction is about 33 Å, together giving 53 Å for the simulation cell size in the $z$ direction. At the beginning of the trajectory, the main center-of-mass motion was away from the surface, and the protein was moving toward the image of the surface. When the protein−surface distance surpassed the nonbonding interaction cutoff, the protein−image surface distance was smaller than it. The protein−image surface attraction then started to play a major role and the scenario seen in the case of simulations with orientation 1 was reproduced, including the protein orientation with respect to the image of the surface. Nevertheless, a simulation with a bigger cell dimension in the $z$ direction might be desirable to check for the possibility of protein rotation, and to explore the time scale to juxtapose its N,C-terminal face. As discussed above, such a simulation would also require a substantially larger cutoff for the nonbonding interactions, and this is beyond our current computational resources.

The surface in orientation 3 induced large protein rotation to expose the N,C-terminal face. From the beginning of the trajectory, C-terminal Arg128 was located close to the surface and its role for adsorption is evident. Other C-terminal residues, e.g., Arg125, were also important. N-terminal residues, e.g., Lys1, Arg5, and Arg14, important for the HEWL−surface adsorption in orientation 1, were located quite far from the surface in orientation 3. However, Lys1 and Arg5 came closer to the surface by about 10 Å. As mentioned in the Results section, HEWL rotation with respect to the surface was the most important feature of the 20 ns trajectory obtained for the HEWL−surface system in orientation 3. It seems that HEWL rotation is driven by the tendency to juxtapose the protein N,C-terminal face to the surface. It is widely accepted that the protein rotation time scale is hundreds of nanoseconds. Hence, the protein rotation and positioning is not complete in the 20 ns simulation and thus the role of the N-terminal residues Lys1 and Arg5 cannot be excluded.

The angle between the major axis of the HEWL ellipsoid and the silica surface in the most interesting trajectory, that for the HEWL−surface system in orientation 1 with an ionic strength of 0.02 M, was about 45°, implying that the protein adsorbs neither end-on nor side-on but somewhere in between. Such a result is consistent with previous observations for HEWL adsorption on thermosensitive nanomagnetic particles[23] and also might elucidate disagreement between the size of protein islands observed in the AFM experiments and the known protein size.[27,30]

**Adsorption on the Nonflat Surface.** As shown in the Results section, the protein in the HEWL−cage system lost its structure during the dynamics. This process was initialized during the heating period. The surface was not flat, and thus, new features upon adsorption were revealed. Nevertheless, in general, all observed trends were consistent with those observed for adsorption on the flat surface. It is worth noting the dipole moment has been oriented toward the corner between walls B1 and B5, so again the dipole moment orientation was compatible with the direction of the movement of the protein's center of mass.

During this trajectory, only two secondary structure elements were not altered at all, $\beta$-structure B1 (residues 43−46) and B2 (residues 51−54). Although all other elements, excluding α-helix A, started to unfold from the beginning of the trajectory, none of them reached a totally unfolded state. This unfolding is an extension of trends observed for the HEWL−surface system in orientation 1 with an ionic strength of 0.02 M (destabilization of α-helix D, α-helix $3_{10}$ from the α-domain, and $\beta$-sheet B3) and is fully consistent with the experimentally observed reduction of the α-helix content,[6,39] as well as the very recent observation that before adsorption on silica nanoparticles wide conformational changes in the lysozyme molecule occur.[60]

On the basis of this, we propose that adsorption on a nonflat surface requires fast and wide conformational rearrangement, much bigger than in the case of adsorption on a flat surface. Such a hypothesis might explain a disagreement in the literature regarding the range of protein conformational changes upon adsorption. As mentioned in the Introduction section, some authors found that HEWL denatures upon adsorption,[33−37] while others found that it does not.[32,38,40] It is possible that the first group of authors had a totally flat surface whereas the second group did not.

Simulations of the protein adsorption on the nonflat surface extended the list of residues important for the protein−surface interactions, caused by the protein denaturation and spreading on the surface. All residues are polar and hydrophilic and just one of them (Gln121) does not possess a charged side chain. Such a set of important residues provides further support for the previous conclusion that the main (monolayer) adsorption driving force is electrostatics. The list of important residues may be divided into two groups. The first one is composed of Lys1, Arg5, Lys13, Arg14, Arg21, Arg112, Lys116, Gln121, Arg125, and Arg128, and the second contains Arg68 and Arg114. Residues from the first group interact with cage wall B5 which is equivalent to the single flat surface in orientation 1, while residues from the second group interact with cage wall B1 perpendicular to wall B5. The first group is located on the N,C-terminal protein face and contains residues found in the case of adsorption on the flat surface. Our second group might be the second adsorption site described by Dismer et al.[22]

We conclude that lysozyme adsorbs most readily on the N,C-terminal face of its surface, and the second site is probably used as a supplementary site when the surface is not flat. The role of

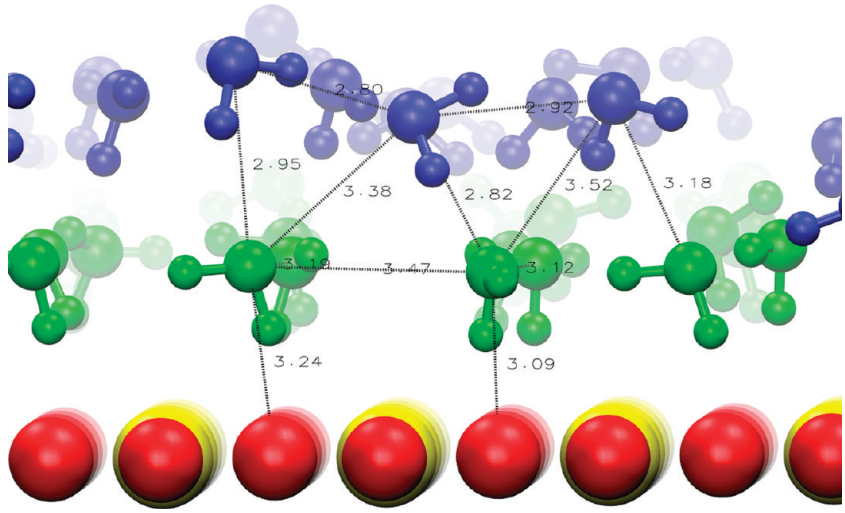


**Figure 8.** Water layers on the surface (view from the side). Surface silicon and oxygen atoms shown as VdW spheres are yellow and red in color, respectively. First and second water layers are shown as green and blue CPKs, respectively. Bulk water is not shown. Some distances are indicated.

arginine residues in the adsorption process is unquestionable. The HEWL protein contains 11 arginines and just three of them, Arg45, Arg61, and Arg73, do not interact with the surface. Since Arg14 and Arg128 interact with the surface even in the trajectory obtained for high ionic strength, we propose that these two residues play the most important role in adsorption. In the case of lysine residues, half of them, Lys33, Lys96, and Lys97, were not important for the attraction to the silica surface.

**Water Layers on the Charged Surface.** As shown in Figure 8, the charged model surface induces the formation of structured water layers. In all of the systems studied, two quite stable water layers were formed in the close proximity of the surface. The distance between surface oxygen and the water oxygen atoms was 3.0−3.2 Å. The distance between water molecules within the same layer was 2.8−3.5 Å (Figure 8). The second water layer was located about 3 Å away from the first layer (Figure 8 and Supporting Information Figure S5), with an extended hydrogen-bond network between the two water layers as well as within each layer. Bulk water was free to interact with the water layers, and water exchange is possible. Water molecules from the outer layer can exchange with water molecules from the inner layer, or from the bulk, with an exchange time scale of ∼16 ps or more. The water molecules from the inner layer are more constrained, and their exchange with bulk water is a two-step, stochastic process. First, they exchange with water molecules from the outer layer and then they can move into the bulk or come back to the inner layer. The initial detachment from the inner layer is not faster than 32 ps. Nevertheless, in all trajectories, it was possible to find inner water molecules which were not exchanged. In the case of the outer layer, all molecules were exchanged on the 20 ns scale. Water molecules which have already moved to the bulk water can return to the outer layer after 1.0 ns of free dynamics in the bulk. Once they reach the outer layer, in the 16 ps time scale, they can return to the inner layer.

Protein adsorption had a visible impact on the water dynamics. Side chains attracted to the surface also stabilized water molecules (via hydrogen bonds) both from the inner and outer layers. For the water molecules adjacent to the side chains, detachment from the outer layer is not faster than 32 ps. If the side chain also penetrates the inner layer (as does Arg128 in some trajectories), at least 120 ps is required for water molecule exchange with the bulk.

During HEWL motion toward the surface, the structured water layers had to be disturbed. In the majority of cases, the protein side chains penetrated just the outer water layer, but sometimes they penetrated both layers. Insertion of one side chain to one water layer was always connected with relaxation of three water molecules from the layer and the creation of a protein−water hydrogen-bond network. Despite the fact that the exchange dynamics of the water involved in the protein−water interactions was strongly slowed down, nevertheless, this effect was rather local and waters located further than 3 Å from the penetrating side chain were not affected much. The kinetics of adsorption, as well as protein motions on the surface, was constrained by the water mobility. Adsorption seems to be easier than protein movement on the surface. The first process is connected with the exclusion of a few water molecules, whereas the second one requires reorganization of water−surface, protein−surface, and protein−water interactions. Adsorbed protein diffusion is therefore strongly constrained by water layers, which provides a possible explanation of the low surface diffusion constant for lysozyme adsorbed on the mica surface.[29−31]

## Conclusions

We have found that protein adsorption strongly depends on the ionic strength and that the dominant interactions driving adsorption are the electrostatic interactions between the charged, hydrophilic surface and HEWL. HEWL adsorption cannot be described simply as a protein landing on the surface. In order to adsorb, the protein has to find the optimal orientation with respect to the surface through protein translations and rotations, which helps explain the adsorption kinetics observed experimentally.[29−31] The range of necessary conformation changes depends on the kind of surface. In the case of the flat surface, conformational changes are rather minor and constrained mainly to the reduction of α-helix content. Adsorption on a nonflat surface requires a loss of the α-helix content as well as protein denaturation. These observations and differences between adsorption on flat and not-flat surfaces might help explain the disagreement in the literature.

In general, our results are in good agreement with previous experimental and computational work; however, our insight into the adsorption process is much more detailed. Despite limitations of the atomistic MD approach, we are able to identify the most

important residues for the adsorption and to describe conformational changes, the sequence of events during adsorption, as well as the protein orientation on the surface. In the 20 ns time scale, we have investigated and clarified the initial events during HEWL adsorption on a charged, hydrophilic surface. Protein diffusion on such a surface, because of its huge time scale, is out of the range of fully atomistic calculations. Nevertheless, other unanswered questions can be addressed, such as the alterations in the protein−protein interactions caused by the presence of the surface, as well as the mechanism governing second layer formation. We are currently working on the preparation of appropriate simulations.

**Acknowledgment.** This work was supported by the UK Engineering and Physical Sciences Research Council through Grant No. EP/E012284. Parts of our results were obtained using the National Service for Computational Chemistry Software (NSCCS) resources, URL: http://www.nsccs.ac.uk.

**Supporting Information Available:** Figures S1-S5 as discussed in the paper. S1 is a side view of the HEWL-cage system. S2 shows the initial and final structures of (a) isolated HEWL with ionic strength 0.5M; (b) HEWL-surface orientation 1 at 0.5M; (c) HEWL-surface orientation 1 at 0.02M using the SPME method; (d) HEWL-surface orientation 2 at 0.02M; (e) HEWL-surface orientation 3 at 0.02M. Figure S3 shows data on the conformational change of the N-terminus for the HEWL-cage system. S4 provides two further views of the HEWL-cage system, (a) as a surface colored by charge and (b) a magnetification of Figure 7. S5 shows a top view of the water layers on the surface. This material is available free of charge via the Internet at http://pubs.acs.org.

## References and Notes

(1) Malmsten, M. *Surfactants and Polymers in Drug Delivery*; Marcel Dekker: New York, 2002.
(2) Kasemo, B. *Surf. Sci.* **2002**, *500*, 656.
(3) Ghoshk, R. *Biochem. Eng. J.* **2003**, *14*, 109.
(4) Moradi, O.; Modarress, H.; Noroozi, M. *J. Colloid Interface Sci.* **2004**, *271*, 16.
(5) Bayramoglu, G.; Yilmaz, M.; Arica, M. Y. *Colloids Surf., A* **2004**, *243*, 11.
(6) Daly, S. M.; Przybycien, T. M.; Tilton, R. D. *Colloids Surf., B* **2007**, *57*, 81.
(7) Adam, N. K. *The physics and chemistry of surfaces*; Oxford University Press: London, 1941.
(8) Blake, C. C. F.; Koenig, D. F.; Mair, G. A.; North, A. C. T.; Phillips, D. C.; Sarma, V. R. *Nature* **1965**, *206*, 757.
(9) Lee-Huang, S.; Huang, P. L.; Sun, Y.; Huang, P. L.; Kung, H.; Blithe, D. L.; Chen, H. C. *Proc. Natl. Acad. Sci.* **1999**, *96*, 2678.
(10) Li, B.; Huang, Y.; Paskewitz, S. M. *FEBS Lett.* **2006**, *580*, 1877.
(11) Garcia Rojas, E. E.; Dos Reis Coimbra, J. S.; Minim, L. A.; Saraiva, S. H.; Sodre de Silva, C. A. *J. Chromatogr., B* **2006**, *840*, 85.
(12) Qiao, S. Z.; Djojoputro, H.; Hu, Q.; Lu, G. Q. *Prog. Solid State Chem.* **2006**, *34*, 249.
(13) Deere, J.; Magner, E.; Wall, J. G.; Hodnett, B. K. *J. Phys. Chem. B* **2002**, *106*, 7340.
(14) Etheve, J.; Dejardin, P.; Boissiere, M. *Colloids Surf., B* **2003**, *28*, 285.
(15) Peng, Z. G.; Hidajat, K.; Uddin, M. S. *J. Colloid Interface Sci.* **2005**, *281*, 11.
(16) Rezwan, K.; Meier, L. P.; Gauckler, L. J. *Biomaterials* **2005**, *26*, 4351.
(17) Lu, J. R.; Su, T. J.; Howlin, B. J. *J. Phys. Chem. B* **1999**, *103*, 5903.
(18) Malmsten, M.; Veide, A. *J. Colloid Interface Sci.* **1996**, *178*, 160.
(19) Shen, D.; Huang, M.; Chow, L.-M.; Yang, M. *Sens. Actuators, B* **2001**, *77*, 664.
(20) Haynes, C. A.; Norde, W. *J. Colloid Interface Sci.* **1995**, *169*, 313.
(21) Bujis, J.; Hlady, V. *J. Colloid Interface Sci.* **1997**, *190*, 171.
(22) Dismer, F.; Petzhold, M.; Hubbuch, J. *J. Chromatogr., A* **2008**, *1194*, 11.
(23) Shamim, N.; Liang, H.; Hidajat, K.; Uddin, M. S. *J. Colloid Interface Sci.* **2008**, *320*, 15.
(24) Su, Y.-L.; Li, Ch. *Appl. Surf. Sci.* **2008**, *254*, 2003.
(25) Peng, Z. G.; Hidajat, K.; Uddin, M. S. *Colloids Surf., B* **2004**, *35*, 69.
(26) Nguyen, T. T.-B.; Chang, H.-Ch.; Wu, V. W.-K. *Diamond Relat. Mater.* **2007**, *16*, 872.
(27) Kim, D. T.; Blanch, H. W.; Radke, C. J. *Langmuir* **2002**, *18*, 5841.
(28) Leisen, F.; Wiechmann, M.; Enders, O.; Kolb, H.-A. *J. Colloid Interface Sci.* **2006**, *298*, 508.
(29) Mulheran, P. A.; Pellenc, D.; Bennett, R. A.; Green, R. J.; Sperrin, M. *Phys. Rev. Lett.* **2008**, *100*, 068102.
(30) Pellenc, D.; Bennett, R. A.; Green, R. J.; Sperrin, M.; Mulheran, P. A. *Langmuir* **2008**, *24*, 9648.
(31) Mulheran, P. A.; Kubiak, K. *Mol. Simul.* **2009**, *35*, 501.
(32) Su, T. J.; Lu, J. R.; Thomas, R. K.; Cui, Z. F.; Penfold, J. *J. Colloid Interface Sci.* **1998**, *203*, 419.
(33) Lu, J. R.; Su, T. J.; Thirtle, P. N.; Thomas, R. K.; Rennie, A. R.; Cubitt, R. *J. Colloid Interface Sci.* **1998**, *206*, 212.
(34) Lu, J. R.; Su, T. J.; Thomas, R. K.; Penfold, J.; Webster, J. *J. Chem. Soc., Faraday Trans.* **1998**, *94*, 3279.
(35) Gidalevitz, D.; Huang, Z.; Rice, S. A. *Proc. Natl. Acad. Sci.* **1999**, *96*, 2608.
(36) Schladitz, C.; Viera, E. P.; Hermel, H.; Mohwald, H. *Biophys. J.* **1999**, *77*, 3305.
(37) Alahverdjieva, V. S.; Grigoriev, D. O.; Ferri, J. K.; Fainerman, V. B.; Aksenenko, E. V.; Leser, M. E.; Michel, M.; Miller, R. *Colloids Surf., A* **2008**, *323*, 167.
(38) Postel, C.; Abillon, O.; Desbat, B. *J. Colloid Interface Sci.* **2003**, *266*, 74.
(39) Yokoyama, Y.; Ishiguro, R.; Maeda, H.; Mukaiyama, M.; Kameyama, K.; Hiramatsu, K. *J. Colloid Interface Sci.* **2003**, *268*, 23.
(40) Larsericsdotter, H.; Oscarsson, S.; Bujis, J. *J. Colloid Interface Sci.* **2004**, *276*, 261.
(41) Romanini, D.; Braia, M.; Angarten, R. G.; Loh, W.; Pico, G. *J. Chromatogr., B* **2007**, *857*, 25.
(42) Clark, A. J.; Kotlicki, A.; Haynes Ch, A.; Whitehead, L. A. *Langmuir* **2007**, *23*, 5591.
(43) Aizawa, T.; Koganesawa, N.; Kamakura, A.; Masaki, K.; Matsuura, A.; Nagadome, H.; Terada, Y.; Kawano, K.; Nitta, K. *FEBS Lett.* **1998**, *422*, 175.
(44) Sauter, C.; Otalora, F.; Gavira, J. A.; Vidal, O.; Giege, R.; Garcia-Ruiz, J. M. *Acta Crystallogr., Sect. D* **2001**, *57*, 1119.
(45) Ravichandran, S.; Talbot, J. *Biophys. J.* **2000**, *78*, 110.
(46) Ravichandran, S.; Madura, J. D.; Talbot, J. *J. Phys. Chem. B* **2001**, *105*, 3610.
(47) Carlsson, F.; Hyltner, E.; Arnebrant, T.; Malmsten, M.; Linse, P. *J. Phys. Chem. B* **2004**, *108*, 9871.
(48) Yokomizo, T.; Higo, J.; Nakasako, M. *Chem. Phys. Lett.* **2005**, *410*, 31.
(49) Hamon, V.; Calligari, P.; Hinsen, K.; Kneller, G. R. *J. Non-Cryst. Solids* **2006**, *325*, 4417.
(50) Calandrini, V.; Hamon, V.; Hinsen, K.; Calligari, P.; Bellissent-Funel, M.-C.; Kneller, G. R. *Chem. Phys.* **2008**, *345*, 289.
(51) Lerbret, A.; Affouard, F.; Bordat, P.; Hedoux, A.; Guinet, Y.; Descamps, M. *Chem. Phys.* **2008**, *345*, 267.
(52) Hery, S.; Genest, D.; Smith, J. C. *J. Mol. Biol.* **1998**, *279*, 303.
(53) Sterpone, F.; Ceccarelli, M.; Marchi, M. *J. Mol. Biol.* **2001**, *311*, 409.
(54) Ionov, R.; Hedoux, A.; Guinet, Y.; Bordat, P.; Lerbet, A.; Affouard, F.; Prevost, D.; Descamps, M. *J. Non-Cryst. Solids* **2006**, *352*, 4430.
(55) McCarthy, A. N.; Grigera, J. R. *J. Mol. Graphics Modell.* **2006**, *24*, 254.
(56) Phillips, J. C.; Braun, R.; Wang, W.; Gumbart, J.; Tajkhorshid, E.; Villa, E.; Chipot, Ch.; Skeel, R. D.; Kale, L.; Schulten, K. *J. Comput. Chem.* **2005**, *26*, 1781.
(57) Humphrey, W.; Dalke, A.; Schulten, K. *J. Mol. Graphics* **1996**, *14*, 33.
(58) Essmann, U.; Perera, L.; Berkowitz, M. L.; Darden, T.; Lee, H.; Pederson, L. *J. Chem. Phys.* **1995**, *103*, 8577.
(59) Kastenholz, M. A.; Hünenberger, P. H. *J. Phys. Chem. B* **2004**, *108*, 774.
(60) Wu, X.; Narsimhan, G. *Biochim. Biophys. Acta* **2008**, *1784*, 1694.

JP901521X